Organic-based microcavities with vibronic progressions: Photoluminescence

L. Mazza*
Max-Planck-Institut für Quantenoptik, Hans-Kopfermann-Straße 1, D-85748 Garching, Germany and Scuola Normale Superiore, Piazza dei Cavalieri 7, I-56126 Pisa, Italy

L. Fontanesi
Institute of Theoretical Physics, Ecole Polytechnique Fédérale de Lausanne (EPFL), CH-1015 Lausanne, Switzerland

G. C. La Rocca
Scuola Normale Superiore and CNISM, Piazza dei Cavalieri 7, I-56126 Pisa, Italy
(Received 14 October 2009; published 15 December 2009)

We theoretically study the photoluminescence properties of organic-based microcavities with vibronic progressions. We analyze the relaxation from the exciton reservoirs to the polariton anticrossing region; the presence of vibronic levels qualitatively enriches the physics of the system with the appearance of new decay channels. The relaxation dynamics is studied with a master equation and the cavity photoluminescence is obtained from the polariton stationary population. We show that the exciton radiative recombination in which a molecule ends up in a vibrationally excited level of the electronic ground state can lead to qualitatively new features in the cavity luminescence spectrum.

DOI: 10.1103/PhysRevB.80.235314 PACS number(s): 78.20.Bh, 71.36.+c, 42.70.Jk

I. INTRODUCTION

The study of the strong light-matter coupling in semiconductor planar microcavities has experienced, in the last decade, the birth of a research field characterized by the use of organic optically resonant media, replacing the inorganic compounds that were employed before. The first experimental studies have been performed using a mixture of J aggregates:[1] even if the organic layer was a highly disordered one, a significantly large oscillator strength brought not only to the formation of polaritonic states but also to a Rabi splitting measurable even at room temperature. Subsequent experimental and theoretical studies have widely inquired the physics of such new systems.[2–6]

More recently, a number of experimental studies have focused their attention on polycrystalline and crystalline materials, featuring a more ordered structure and optical properties usually dominated by vibronic progressions. The growth of very ordered samples, up to the very recent creation of anthracene-based single-crystal microcavities,[7,8] has allowed the observation of different phenomena arising from the strong optical anisotropy of organic crystals.[9–12] On the other side, vibronic replicas have been strongly coupled to light, with the consequent observation of three (or more) polariton dispersion relations.[13]

Here, we continue the theoretical study of organic-based microcavities started in a previous work,[14] in which we focused our attention on the consequences deriving from the presence of vibronic replicas. There we have analyzed the linear optical properties of these heterostructures; we introduced both a quantum approach and a semiclassical one and used them to study the reflectivity and transmittivity of the microcavity.[15] We showed that a theoretical model accounting for the possibility of strong coupling between light and vibronic levels can satisfactorily explain the data reported in Ref. 13.

Here, we focus on the photoluminescence properties of these microcavities under nonresonant pumping conditions. A master equation is set up and used to study the evolution of the population of the polariton states; the stationary population is then linked to the measured photoluminescence through a simple model for the cavity mirrors. Among the many processes involving vibronic replicas, we found that the radiative recombination of excitons in which a molecule ends up in a vibronically excited level of the electronic ground state is that with the most significant qualitative consequences. Indeed, this process gives rise to a polariton scattering rate that selectively populates polaritonic states whose energy is lower than that of the exciton reservoir of one (or more) molecular vibronic quantum (quanta).

This paper is organized as follows: in Sec. II the theoretical model is exposed and in Sec. III some numerical simulations are shown. Finally, in Sec. IV our conclusions are presented.

II. THEORETICAL MODEL

In this section the theoretical model for the study of the cavity photoluminescence will be illustrated. We focus on organic-based microcavities whose optical medium has an ordered internal structure; molecules are also assumed to feature vibronic progressions in absorption and luminescence. Photoluminescence data for a similar microcavity have already been published; in Ref. 12 an experimental angle-resolved analysis of the photoluminescence properties of a crystalline anthracene-based microcavity has been reported; as shown in Ref. 7, where the same system was studied, this material exhibits optically active vibronic replicas. The presence of two molecules per unit cell leads to the splitting of the lower polariton branch into two branches, from which the luminescence has been collected.

However, our theoretical study is not aimed at reproducing specific data or experiments and the model we develop is rather general in its nature. The illustrative numerical simu-

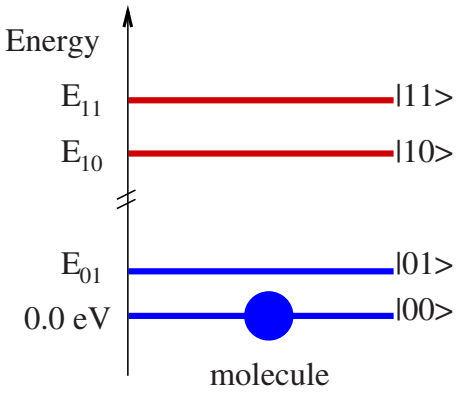

FIG. 1. (Color online) Sketch representing the energy levels of the molecule composing the organic crystal. Usually $E_{10} \gg E_{01}$ and $E_{11}-E_{10} \sim E_{01}$.

lations presented below are obtained exploring some physically meaningful parameter ranges with the aim of investigating the main consequences of the new relaxation processes. The simplest case of a single molecule per unit cell is here considered to show the qualitatively new features due to the vibronic replicas.[16,17]

The theoretical study of the photoluminescence comprises three main steps. In the first one (Sec. II A), we identify the real eigenstates of the system, i.e., the polaritons. In the second step (Sec. II B), we focus on the weaker interactions responsible for the polariton relaxation; they will be treated within a Fermi golden-rule approach and described by polariton scattering rates. Finally, we set up a master equation describing the dynamical polariton relaxation (Sec. II C); from its solutions it will be possible to extract information about the microcavity luminescence. In the following, for the sake of simplicity, we explain the model for a molecule with only one vibronic replica both at the ground and excited states, as in Fig. 1; the model can be easily generalized to an arbitrary number of them.

A. Polaritons

If we consider a strongly coupled microcavity, the eigenstates of the system are the polaritons, i.e., the eigenstates of the light-matter interaction involving the $|00\rangle \leftrightarrow |1n\rangle$ transitions [see the quantum model presented in Ref. 14 and Figs. 2(a) and 2(b)]. We assume the vibrational energy quantum to be significantly larger than $k_B T$ at room temperature and therefore the $|01\rangle$ states have a negligible thermal population. This means that absorption along $|01\rangle \rightarrow |1n\rangle$ channels is immaterial and thus the corresponding polariton states do not form, i.e., the $|01\rangle \leftrightarrow |1n\rangle$ transitions cannot strongly couple to light. We could ask whether a long succession of photoluminescence processes might be able to create a large $|01\rangle$ population, such that absorption could eventually take place. We should first be aware that the $|01\rangle$ level has a short lifetime on the order of 1–100 fs.[18] Furthermore this accumulating population has never been seen by experiments performed on samples out of cavity and even if the light-matter interaction is enhanced by the cavity mirrors, we neglect the possibility of absorption from the $|01\rangle$ level and the corresponding polaritons.

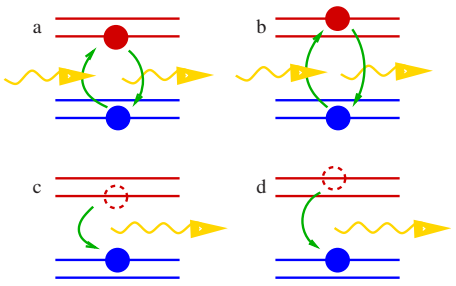

FIG. 2. (Color online) Sketch representing the interaction of the molecule with light. The interaction of photons with $|00\rangle \leftrightarrow |10\rangle$ and $|00\rangle \leftrightarrow |11\rangle$ transitions gives rise to polaritons [(a) and (b)]. Since the absorption from the $|01\rangle$ level is almost immaterial, the photoemission from the $|10\rangle \rightarrow |01\rangle$ and $|11\rangle \rightarrow |01\rangle$ transitions works as a polariton relaxation channel [(c) and (d)].

B. Polariton relaxation

We now model the main processes responsible of polariton relaxation and describe each of them through a scattering rate. First of all, we consider all those light-matter processes not contributing to the polariton formation, i.e., molecular photoluminescence transitions ending in a $|01\rangle$ level [Figs. 2(c) and 2(d)]. The light-matter interaction is still studied through the dipole approximation, $V^{lm} = -\boldsymbol{\mu} \cdot \mathbf{E}$, taking into account transitions that have been neglected in the quantum approach in Ref. 14. If we consider, for instance, s-polarized light and the transitions $|10\rangle \rightarrow |01\rangle$ of a molecule located in $\mathbf{n}$, the potential takes the form (the result can be easily generalized to other light polarization and molecular transitions)

$$V^{lm}_{\mathbf{n}} = -i \sum_{\mathbf{q}} \sum_{\mathbf{k}} \sqrt{\frac{4\pi\hbar\omega_{\mathbf{q}}}{LA\varepsilon}} \sqrt{\frac{2}{M(N+1)}} \times (-\sqrt{S}) \frac{e^{-S/2}}{\sqrt{\mathcal{N}}} \mu_x \sin\phi \sin\left[\frac{\pi n_z}{a(N+1)}\right] \times e^{i(\mathbf{q}-\mathbf{k})\cdot\mathbf{n}_{\parallel}} [v_{01,\mathbf{n}} b^{\dagger}_{0,\mathbf{k}} a_{s,\mathbf{q}} + \text{H.c.}], \quad (1)$$

where $v^{\dagger}_{01,\mathbf{n}}$ is the operator that creates a vibronic replica at the ground state; in this formula and in the next ones the dipole is oriented along the $\hat{x}$ axis.

Then we consider the scattering process mediated by a molecular photoemission with creation of a vibronic replica at the ground state starting from a polariton $|A^i_{\mathbf{k}}\rangle$ and ending in a polariton $|A^j_{\mathbf{q}}\rangle$: if we sum over all the molecules mediating this process, we get the scattering rate,

$$W^{(lm)}_{i,\mathbf{k}\rightarrow j,\mathbf{q}} = \sum_{\mathbf{n}} W^{(lm)}_{\mathbf{n}i,\mathbf{k}\rightarrow j,\mathbf{q}} = \frac{2\pi}{\hbar} \frac{4\pi\hbar\omega_{\mathbf{q}}}{LA\varepsilon} \frac{e^{-S}}{\mathcal{N}} \mu_x^2 \left| iX^{j*}_{s\mathbf{q}} \sin\phi + X^{j*}_{p\mathbf{q}} \sqrt{1 - \frac{|\mathbf{q}|^2}{|\mathbf{q}|^2 + q_z^2}} \cos\phi \right|^2 |-\sqrt{S} X^i_{0\mathbf{k}} + X^i_{1\mathbf{k}}|^2 \delta[E^i(\mathbf{k}) - E^j(\mathbf{q}) - E_{01}]. \quad (2)$$

The main peculiarity of this expression is the last energy-conserving delta function, forcing the involved polaritons to have an energy difference equal to the vibronic quantum E_{01}; on the other side, since the scattering is mediated by a process localized on single molecules, the in-plane momentum is not conserved. This expression has been obtained assuming that the final vibrational state is localized onto the single molecule mediating the process.

We then consider the interaction of each molecule with its reservoir of low-energy degrees of freedom, i.e., the fact that, when electronically excited, they can release/take some energy to/from environmental degrees of freedom [represented by the $w_{\mathbf{n}}^{\dagger}(\omega)$ and $w_{\mathbf{n}}(\omega)$ operators]. We can describe this process as a weak linear interaction term,

$$V_{\mathbf{n}}^{(1)} = [\mathcal{W}_{10} b_{0,\mathbf{n}}^{\dagger} b_{0,\mathbf{n}} + \mathcal{W}_{11} b_{1,\mathbf{n}}^{\dagger} b_{1,\mathbf{n}}] \times \int [w_{\mathbf{n}}^{\dagger}(\omega) + w_{\mathbf{n}}(\omega)] \rho_w(\omega) d\omega, \tag{3}$$

where $\mathcal{W}$ has the dimensions of an energy and represents the coupling strength; $\rho_w(\omega)$ is the reservoir density of states. If we consider the scattering rate mediated by this process, we get

$$W_{i,\mathbf{k}\to j,\mathbf{q}}^{(1)} = \sum_{\mathbf{n}} W_{\mathbf{n}i,\mathbf{k}\to j,\mathbf{q}}^{(1)} = \frac{1}{\tau^{(1)}} \frac{3}{2M(N+1)} \cdot |X_{0\mathbf{q}}^{j*} X_{0\mathbf{k}}^{i} + X_{1\mathbf{q}}^{j*} X_{1\mathbf{k}}^{i}|^2. \tag{4}$$

To derive Eq. (4), we have assumed $\mathcal{W}_{10}$ and $\mathcal{W}_{11}$ to be equal to the same value $\mathcal{W}$ and the density of final states to be frequency-independent ρ_w; these approximations are justified since we are developing an effective "qualitative" model and more involved assumptions would imply the introduction of additional new parameters, as discussed before. The scattering time is equal to $\tau^{(1)} = \frac{|\mathcal{W}|^2}{\hbar} \frac{\rho_w}{\hbar}$ and will be estimated in the following. If the final polariton has a lower energy with respect to the initial one, this formula is correct in the approximation that the population of the degrees of freedom n_{dof} is very small $(1+n_{dof} \approx 1)$. When considering scattering to a final polariton having a larger energy, instead, we should only multiply this formula by the thermal population of the degrees of freedom; this strongly decreases the relevance of these processes.

Vibronic replicas are not stable states. They interact with a reservoir of low-energy degrees of freedom, this causing their relaxation to lower-lying vibronic states. As before, we model this interaction with a weak linear coupling between vibronic states and the reservoir; after some manipulation similar to that presented for the previous scattering process we get the following expression:

$$W_{i,\mathbf{k}\to j,\mathbf{q}}^{(2)} = \frac{1}{\tau^{(2)}} \frac{3}{2M(N+1)} |X_{0\mathbf{q}}^{j}|^2 |X_{1\mathbf{k}}^{i}|^2. \tag{5}$$

As before, the formula refers to the case with the final polariton state having an energy lower than that of the initial one; if this is not the case, the formula must be multiplied by the thermal population of the degrees of freedom. The scattering time $\tau^{(2)}$ is the only free parameter of this expression.

The last process we have to take into account is the photon leakage through the microcavity mirrors. This effect can be effectively described within the quasimode approximation, introduced within the quantum approach in Ref. 14. The polariton escape rate from the microcavity to the external photon modes takes the following form:

$$W_{i,\mathbf{k}\to ext,\mathbf{k}}^{qm} = \gamma_{pht} \sum_{\lambda} |X_{\lambda\mathbf{k}}^{i}|^2. \tag{6}$$

C. Master equation

A master equation describes the time evolution of the population of one specific polariton in terms of the incoming and outcoming rates. If we define the total polariton scattering rate as

$$\tilde{W}_{i,\mathbf{k}\to j,\mathbf{q}} = W_{i,\mathbf{k}\to j,\mathbf{q}}^{(lm)} + W_{i,\mathbf{k}\to j,\mathbf{q}}^{(1)} + W_{i,\mathbf{k}\to j,\mathbf{q}}^{(2)}, \tag{7}$$

the master equation reads

$$\dot{n}_{i,\mathbf{k}} = \sum_{j,\mathbf{q}} (\tilde{W}_{j,\mathbf{q}\to i,\mathbf{k}} n_{j,\mathbf{q}} - \tilde{W}_{i,\mathbf{k}\to j,\mathbf{q}} n_{i,\mathbf{k}}) + - W_{i,\mathbf{k}\to ext,\mathbf{k}}^{qm} n_{i,\mathbf{k}} + P_{i,\mathbf{k}}, \tag{8}$$

where $P_{i,\mathbf{k}}$ represents the pumping term. We solve this rate equation looking for the steady state, i.e., we suppose that the pumping pulse duration is long enough to allow the polariton population to relax to the stationary value. We then put $\dot{n}_{i,\mathbf{k}} = 0$ and obtain a simple linear system, numerically solved with standard linear-algebra routines, that gives us the steady populations $\tilde{n}_{i,\mathbf{k}}$.

Photoluminescence is calculated as the number of emitted photons per unit time. We stress that each internal polariton is interacting with a continuum of external modes labeled by ω; we consider a Lorentzian broadening around the energy of the polariton with linewidth γ_{exc} for the excitonic participation and γ_{pht} for the photon one. The total frequency-density photoluminescence at given $\mathbf{k}$ is the sum of the contribution coming from all the polaritons sharing the same $\mathbf{k}$,

$$\sum_{i} f_{i,\mathbf{k}}(\omega) = \sum_{i} W_{i,\mathbf{k}\to ext,\mathbf{k}}^{qm} \tilde{n}_{i,\mathbf{k}} \rho_{i,\mathbf{k}}(\omega), \tag{9}$$

where $\rho_{i,\mathbf{k}}(\omega)$ is the Lorentzian luminescence spectral shape mentioned above.

The study of the photoluminescence under nonresonant pumping conditions will be carried out by "pumping" the pure excitonic high-$|\mathbf{k}|$ states (or exciton reservoir). This is an effective description of what happens when the laser incoherently excites the high-energy degrees of freedom of the microcavity; after a fast relaxation, they decay to lower-lying states, i.e., polaritons in the anticrossing region and excitons in the reservoirs. Since, as it will be estimated in the next section, the number of excitons is much larger than the number of polaritons, we can effectively describe the process of nonresonant pumping as an incoherent population of the exciton reservoir. Indeed, the population of the polariton states will then be ruled by the excitations decaying from the exciton reservoir into the anticrossing region. In the following simulations, $P_{i,\mathbf{k}}$ will be set different from zero only for the exciton reservoir states.

Before going on, we want to finally discuss the photoluminescence model for J aggregates proposed by Litinskaya *et al.* in Ref. 19. In their study, focused on J-aggregate-based microcavities, they considered the polariton scattering mediated by a molecular optical phonon and estimated the rate of this relaxation channel around 10–25 ps. Such an estimate can be carried out also for anthracene-based microcavities and gives a larger result of around 100 ns, a significantly larger lifetime due to the larger density of the medium; therefore we do not explicitly consider this process.

III. NUMERICAL SIMULATION

A. Parameters

We start with a brief discussion of the main parameters used in the simulation. We are interested in describing a generic system, and therefore the parameters are only chosen to fit the main features of organic materials; they will be different from those needed to simulate the system in Ref. 12 or from those used in Ref. 14 addressing the experimental results presented in Ref. 13. Nevertheless, a fast check shows that parameters used in the previous section are comparable to those listed here below, hence the results presented in the following can also be applied in their qualitative features to the previous specific setup.

Cavity features. We simulate a microcavity of length 2000 Å. The cavity is filled with a material of dielectric constant $\varepsilon=3.0$, the crystal layer is put exactly in the middle of the microcavity. We assume it to have a cubic Bravais lattice, with lattice constant $a=15$ Å. We stress that we consider the simplest system with only one molecule per unit cell because we want to focus our attention only on the effects of vibronic replicas.

Photon linewidth. A typical photon linewidth varies from 0.01 to 0.03 eV for microcavities reaching reflectivity values larger than 95%. The relative photon lifetimes vary, respectively, from 150 to 50 fs. In the simulations the intermediate value of 0.02 eV was employed.

Molecular energy levels. The ground-state energy is set to 0.0 eV. In the following, the excited-state energy will vary from 1.9 to 2.0 eV. We stress that due to the intermolecular interactions the crystal resonance is slightly lower (see the Hamiltonian of the quantum approach in Ref. 14). We use as molecular dipole strength $\mu_{\|}=2.8\sqrt{\text{eV Å}^3}=3.5$ D.

Exciton linewidth. We consider an effective linewidth γ_{exc} including both the homogeneous and inhomogeneous broadenings. In the next simulations we mainly use the value $\gamma_{exc}=0.1$ eV, compatible with the linewidth of the absorbance of 3,4,7,8 napthalenetetracarboxylic dianhydride (NTCDA) in Ref. 13 and anthracene in Ref. 7. We stress that this is the only way disorder is taken into account in our model.

Relaxation time. It is difficult to set a proper value for the relaxation time $\tau^{(1)}$ since we developed an effective model. We estimate this parameter looking at the results it gives; in Ref. 4 the ratio between the peak intensities is within the range of 1–10 %, which we managed to reproduce with a $\tau^{(1)}\sim 100-500$ fs (not shown). The use of the measures presented in Ref. 12 is more problematic since the luminescence coming from two split lower branches is observed, a feature that is not included in our model. As far as the fast vibronic relaxation is considered, we set $\tau^{(2)}=100$ fs.[18]

In usual cavity situations, the anticrossing region does not extend beyond $|\mathbf{k}|=0.001$ Å^{-1}, i.e., remains within the zone covered by typical mirror stop band; for larger values there would be no cavity photons and thus polaritonic phenomena could not occur. However, the first Brillouin zone is much larger than the anticrossing region and we can give a simple estimate of this. The area of the anticrossing region is

$$\mathcal{A}_{anticrossing}=\pi(0.001)^2 \text{ Å}^{-2}\sim 3\times 10^{-6} \text{ Å}^{-2} \tag{10}$$

whereas the area of the first Brillouin zone is

$$\mathcal{A}_{BZ}=\left(\frac{2\pi}{a}\right)^2=\frac{4\pi^2}{15\times 15} \text{ Å}^{-2}\sim 10^{-1} \text{ Å}^{-2} \tag{11}$$

so that the latter is more than four order of magnitude larger than the first.

When dealing with scattering processes, we cannot neglect the presence of such a large quantity of excitations. Inside the anticrossing region, the correct way to deal with the excitations belonging to the one-excitation manifold is to work within the polariton framework. Outside the anticrossing region, we must only consider pure excitonic states acting as a reservoir since their scattering rates to and from other excitations are the same. In that region photons are going to play a negligible role due to the lower reflectivity of mirrors at such incidence angles and to the fact that they are too high in energy to significantly interact with excitons. From a computational point of view since we are not interested in the population of each of these excitons but only in how their presence affects the polariton population evolution, we define a pseudostate whose population is the sum of the populations of these excitons. Scattering rates from this pseudostate are the same as before whereas each scattering rate to this pseudostate is the product of the number of reservoir excitons times the corresponding scattering rate to one of the excitons.

On the other hand, polaritons inside the anticrossing region have very different features, due to the dependence of the $X^t_{\lambda\mathbf{k}}$'s and $X^t_{j\mathbf{k}}$'s both on the absolute value $|\mathbf{k}|$ and on the angle ϕ between the propagation direction and the axis $\vec{\mu}_{\|}$ is pointing along. The dependence on $|\mathbf{k}|$ can be easily taken into account by partitioning the anticrossing region into concentric rings, as it is usually done in isotropic systems. Our anisotropic sample would in addition require a further partitioning into circular sectors, since, as it is stated in the quantum approach of Ref. 14, the polarization of the photon coupling to the matter depends on ϕ. The problem arises because the s and p polarizations couple to the electronic excitations in a different way and this, for instance, makes all the scattering rates involving molecular photoemission to the $|01\rangle$ level depend on ϕ.

However, we want here to show that these differences are small. If we assume that the total photon participation $|X^t_{s\mathbf{k}}|^2+|X^t_{p\mathbf{k}}|^2$ is independent of ϕ, then the ratio between the s and p light-matter couplings

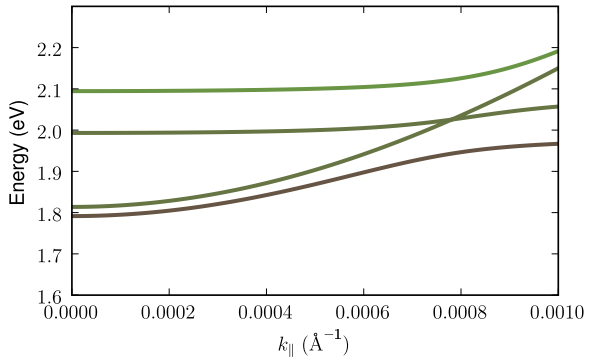

FIG. 3. (Color online) Dispersion relations of the normal propagating modes for the microcavity considered in the numerical simulation. The organic active layer is constituted by molecules with one vibronic replica both at the electronic ground and excited states, as depicted in Fig. 1. Photons whose polarization is parallel to the dipole interact with excitons and give rise to three polariton branches, the third arising from the interaction with the vibronic level $|11\rangle$. The middle photonlike dispersion relation represents the other photon polarization.

$$\frac{g_{jp\mathbf{k}}}{g_{js\mathbf{k}}} = \sqrt{1 - \frac{|\mathbf{k}|^2}{|\mathbf{k}|^2 + \frac{\pi^2}{L^2}}} \tag{12}$$

varies between 1 at $|\mathbf{k}|=0$ and 0.86 at the boundary of the anticrossing region. Therefore, being the difference between $g_{jp\mathbf{k}}$ and $g_{js\mathbf{k}}$ small, we effectively treat the ring as a single state and do not partition the region into circular sectors. We stress that this assumption is not equivalent to treating the system as isotropic; there will always be an uncoupled photon and a coupled one; we simply do not keep track of their specific polarizations around the ring. This approximation is not going to qualitatively affect the results but only to bring about small quantitative changes. Hence, a single polariton for each $|\mathbf{k}|$ will represent all the polaritons with the same $|\mathbf{k}|$, but with different propagation directions, and we take as a representative the low-symmetry polariton with $\phi=\pi/4$.

B. Results

We now present the results of a numerical simulation in which we studied the photoluminescence of a microcavity with the model exposed in the previous section. We consider as cavity active layer a crystal whose molecules have one vibronic replica at the ground state and one vibronic replica at the excited state (Fig. 1). The additional level $|11\rangle$ behaves as a new resonance and thus a new polariton appears, as discussed in Refs. 13 and 14. The dispersion relations are showed in Fig. 3. Apart from the three polariton dispersion relations, an uncoupled photon mode is recognizable; this is the signature of the anisotropy of the medium.[10,11]

TABLE I. Main computational parameters used in the simulation.

Molecular levels	$\|00\rangle$, $\|10\rangle$, $\|01\rangle$, $\|11\rangle$
E_{10}	1.97 eV
E_{01}	0.1 eV
E_{11}	1.97+0.1 eV
γ_{exc}	0.1 eV
γ_{pht}	0.02 eV
$\tau^{(1)}$	500 fs
$\tau^{(2)}$	100 fs

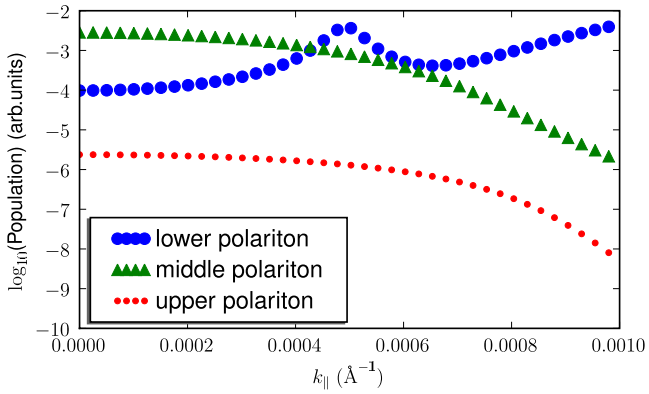

FIG. 4. (Color online) Stationary polariton populations of the simulated system. The lower polariton features *e* population peak at around 5×10^{-4} Å^{-1}.

We expect all the scattering processes considered in the previous section to be effective; the intrabranch scattering, the replica relaxation, and the exciton radiative recombination with creation of one vibration at the ground state. The parameters used in the simulation are shown in Table I. As previously discussed, nonresonant pumping is mimicked injecting population into the exciton reservoir.

Figure 4 shows the stationary polariton populations. The most interesting feature is the peak featured by the lower polariton population at about 5×10^{-4} Å^{-1}. This peak is going to play an important role once the photoluminescence is considered; Figs. 5 and 6 show a luminescence peak coming from the lower polariton at around 5×10^{-4} Å^{-1}. The presence of this peak derives from polariton scattering mediated by the exciton radiative recombination with molecule ending in the $|01\rangle$ state. Since, due to energy conservation, the final "polariton+vibration" state must have as a whole the energy of the initial polariton, the final polariton has always the energy of the initial one minus E_{01}, that is a fixed value. The population peak is due to the large scattering from the lower exciton reservoir to states with an energy lower of E_{01}, in our case 0.1 eV.

We have performed other simulations varying some internal and external parameters (not shown here) even if the results differ in they quantitative features and in the exact form of the line shapes, the appearance of the population and luminescence peaks due to the presence of ground vibronic replicas always takes place. Hence, the main result of these simulations, a polariton relaxation process very effective in selectively populating a part of the lower branch, is not a result depending on the tuning of computational parameters.[20] We think that by a proper choice of cavity detuning and Rabi splitting it could also be effectively used

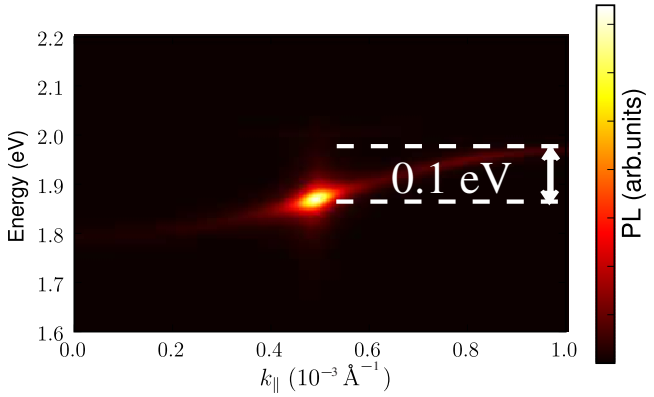

FIG. 5. (Color online) Pictorial representation of the photoluminescence coming from the simulated microcavity. The luminescence features a peak in the lower polariton branch that is due to the radiative recombination of the excitons in the lower reservoir. An explicit signature of such a process is the energy difference between the peak and the reservoir, that must be equal to a vibronic quantum E_{01}.

as a tool to populate the bottom region at $\mathbf{k}=0$ of the lower branch, a process crucial to achieve polariton Bose-Einstein condensation (BEC).[21]

The whole discussion has been carried out studying the stationary population of the system since we were assuming that the pump pulse was long enough to let the system reach the stationary state. As a matter of fact, the pump, acting as a population source for the exciton reservoir, injects energy inside the cavity, changing only the total number of excitations but not their distribution among the different polariton states which determines the photoluminescence spectral shape and is only due to the linear scattering rates appearing in Eq. (8). The stationary value of the total number of excitations is simply due to a balance between the rate of ejected photons and that of injected reservoir excitons. A more complex situation would have been the complete study of nonresonant pumping, considering also the initial fast relaxation of high-energy levels excited by the laser. This means that the luminescence spectral shape can be described by Eq. (8) only after the time needed by the high-energy excitations to decay to the exciton reservoir states.

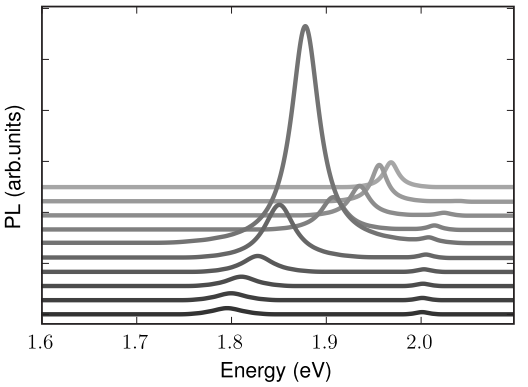

FIG. 6. Pictorial representation of the photoluminescence coming from the simulated microcavity. Each solid line represents the luminescence spectrum at definite $\mathbf{k}$ vector. The darkest one is taken at $|\mathbf{k}| \sim 0$ Å^{-1} whereas the lightest one is taken at $|\mathbf{k}| \sim 0.001$ Å^{-1}. It is possible to recognize light coming from middle polariton branch, as well as the peak from the lower polariton.

IV. CONCLUSIONS

In this paper we focused on the photoluminescence properties of organic-based microcavities with vibronic progressions. A theoretical model has been developed in order to give an insight into the effects of the new decay channels due to the presence of molecular vibronic levels. With the help of a master equation the dynamical evolution of the polariton relaxation has been simulated and some numerical results have been shown, where the presence of vibronic replicas at the molecular ground state has proved to be source of interesting qualitative features. In particular, molecular photoluminescence processes ending in a $|0n\rangle$ state lead to a polariton scattering process very effective in selectively populating low-energy regions of the lower polariton branch.

ACKNOWLEDGMENTS

We would like to thank Paolo Michetti, Vincenzo Savona, Wolfgang Langbein, and Stephane Kéna-Cohen for fruitful discussions and comments on this work during its preparation. We gratefully acknowledge support of the European Commission via Grant No. FP7-PEOPLE-ITN-2008-237900 "ICARUS."

*leonardo.mazza@mpq.mpg.de

[1] D. G. Lidzey, D. D. C. Bradley, M. S. Skolnick, T. Virgili, S. Walker, and D. M. Whittaker, Nature (London) **395**, 53 (1998).
[2] D. Lidsey, in *Thin Films and Nanostructure*, edited by V. Agranovich and G. Bassani (Elsevier, New York, 2003), Vol. 31.
[3] V. Agranovich and G. C. La Rocca, Solid State Commun. **135**, 544 (2005).
[4] P. Michetti and G. C. La Rocca, Phys. Rev. B **77**, 195301 (2008).
[5] P. Michetti and G. C. La Rocca, Phys. Rev. B **79**, 035325 (2009).
[6] V. Agranovich, *Excitations in Organic Solids* (Oxford University Press, New York, 2009).
[7] S. Kéna-Cohen, M. Davanço, and S. R. Forrest, Phys. Rev. Lett. **101**, 116401 (2008).
[8] H. Kondo, Y. Yamamoto, A. Takeda, S. Yamamoto, and H. Kurisu, J. Lumin. **128**, 777 (2008).
[9] S. Kéna-Cohen and S. R. Forrest, Phys. Rev. B **77**, 073205 (2008).
[10] M. Litinskaya, P. Reineker, and V. M. Agranovich, Phys. Status Solidi A **201**, 646 (2004).
[11] H. Zoubi and G. C. La Rocca, Phys. Rev. B **71**, 235316 (2005).
[12] S. Kéna-Cohen, M. Davanço, and S. R. Forrest, Phys. Rev. B **78**, 153102 (2008).
[13] R. J. Holmes and S. R. Forrest, Phys. Rev. Lett. **93**, 186404 (2004).

[14] L. Fontanesi, L. Mazza, and G. C. La Rocca, preceding paper, Phys. Rev. B **80**, 235313 (2009).
[15] L. Fontanesi and G. C. La Rocca, Phys. Status Solidi C **5**, 2441 (2008).
[16] L. Fontanesi, L. Mazza, and G. C. La Rocca, Proceeding of ICPS 29, 2008 (unpublished).
[17] L. Mazza, M.S. thesis, University of Pisa, 2008.
[18] M. Pope and C. E. Swenberg, *Electronic Processes in Organic Crystals and Polymers* (Oxford University Press, New York, 1999).
[19] M. Litinskaya, P. Reineker, and V. M. Agranovich, J. Lumin. **110**, 364 (2004).
[20] While writing this paper we have been informed (S. Kéna-Cohen, private communication, 2009) that this new effect has been recently measured in crystalline anthracene-based microcavities and that measures with different cavity detuning have been performed, all supporting the presence of a strong scattering phenomenon from the exciton reservoir to the polariton states whose energy is lower of a vibrational quantum.
[21] J. Kasprzak, M. Richard, S. Kundermann, A. Baas, P. Jeambrun, J. M. J. Keeling, F. M. Marchetti, M. H. Szymańska, R. André, J. L. Staehli, V. Savona, P. B. Littlewood, B. Deveaud, and L. S. Dang, Nature (London) **443**, 409 (2006).